64

SOCIETY OF AUTOMOTIVE ENGINEERS, INC.
400 Commonwealth Drive, Warrendale, Pa. 15096

A Performance Model for the Texaco Controlled Combustion, Stratified Charge Engine

B. C. Jain, J. M. Rife, and J. C. Keck
Massachusetts Institute of Technology

SOCIETY OF AUTOMOTIVE ENGINEERS

Automotive Engineering Congress and Exposition
Detroit, Michigan
February 23-27, 1976

760116

760116

A Performance Model for the Texaco Controlled Combustion, Stratified Charge Engine

B. C. Jain, J. M. Rife, and J. C. Keck
Massachusetts Institute of Technology

THE TERM STRATIFIED charge engine is generally accepted to describe a spark-ignition, internal combustion engine with a non-uniform fuel-air mixture in the combustion chamber. With the increased emphasis on both exhaust emissions and fuel economy over the past few years, interest in the stratified charge engine has risen dramatically and various approaches for stratification of the fuel-air mixture have been studied in depth. In this paper, we discuss a performance model for the Texaco direct injection stratified charge engine. The Texaco Controlled Combustion System (TCCS) demonstrates excellent fuel economy, broad fuel tolerance and relatively low emissions.

The basic conceptual details behind the Texaco Controlled Combustion System are described below and additional details can be found in the references on the TCCS engine (1-4).**

TCCS ENGINE DESCRIPTION

The Texaco Controlled Combustion System is illustrated schematically in Figure 1. A high air swirl is induced by the flow through the inlet valve and is amplified during compression by the combustion chamber configuration. The combustion chamber is a cup in the piston with a cylindrical upper section and toroidal bottom. The diameter of the cup is approximately one half of the cylinder

*With the assistance of E. Mayer, Texaco and W. Bryzik, U.S. Army Tank-Automotive Systems Development Center.

**Numbers in parentheses refer to the list of references.

ABSTRACT

A model has been developed to predict the performance of the Texaco Controlled Combustion, Stratified Charge Engine starting from engine geometry, fuel characteristics and the operating conditions. This performance model divides the engine cycle into the following phases: Intake, Compression, Rapid Combustion, Mixing-Dominated Expansion, Heat-Transfer Dominated Expansion and Exhaust. During the rapid combustion phase, the rate of heat release is assumed to be controlled by the rate of fuel injection and the air-to-fuel ratio. The burning rate in the mixing controlled stage appears to be dominated by the rate of entrainment of the surrounding gas by the plume of burning products and this rate is assumed to be controlled by the turbulent eddy entrainment velocity.

A plume geometry model has been developed to obtain the surface area of the plume for entrainment during the mixing dominated phase. The model also gives the wall areas in contact with the hot, burned gas plume and the relatively cold unburned gas for heat transfer calculations.

Comparison of the model predictions with the available experimental data shows good agreement. In addition, the potential of the performance model as a design tool is demonstrated with a parametric analysis.

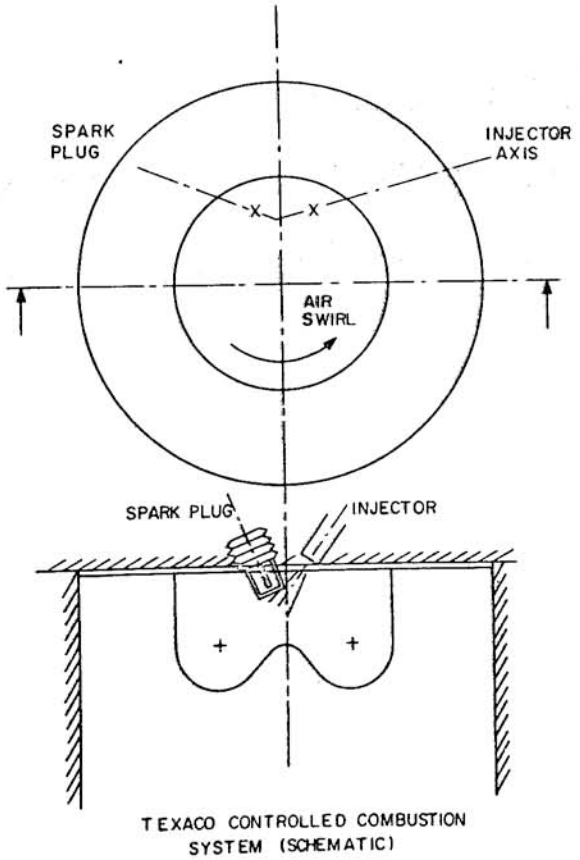

Fig.1 - Texaco Controlled Combustion System (schematic)

diameter.

The high pressure injection system is based on diesel engine components and uses a Roosa Master Pencil Nozzle. The distinguishing feature of this nozzle is a flat seat and a single-hole orifice instead of the more common conical seating, multiple-hole sac-tip design. All of the remaining details are essentially equivalent to the standard production nozzle. Valve opening pressure is typically set at 1500-2000 psi. The ignition system developed for the engine, referred to as the Texaco Ignition System (TTIS), is a high energy, multi-discharge unit with controlled spark duration (5).

Fuel is injected near the end of the compression stroke, and the fuel jet entrains air as it penetrates from the injection to the spark plug. The first increment of fuel is ignited as it reaches the spark plug and a flame-front is established immediately downstream of the spark plug. As fuel injection continues, additional fuel and air reach the flame-front at the spark plug and the fuel is burned almost as rapidly as it is injected. In full load operation the fuel injection interval corresponds approximately to the time for one air swirl and the overall air-fuel ratio is near stoichiometric. Lower loads are obtained by decreased fuel injection duration and quantity, consequently the overall air-fuel ratio at part load is lean and may approach 100:1 at idle conditions.

Typical diesel engine problems of long ignition delay, high rates of pressure rise and high peak pressures with low cetane fuels and low compression ratios are avoided in TCCS operation by providing a positive ignition source. The problems of spontaneous ignition and octane requirement associated with conventional gasoline engines are also eliminated with TCCS since the residence time of combustible fuel-air mixtures in the combustion chamber is extremely short.

In summary, the TCCS mode of operation results in several unique characteristics including high part-load thermal efficiency at lean mixtures and inherently low hydrocarbon and carbon monoxide emissions resulting from excess air operation and controlled combustion rates. In addition, with the high pressure injection system, a wide range of fuel volatility can be tolerated with no apparent sensitivity to either the octane or cetane number of the fuel. These characteristics, in addition to quick warm-up and excellent driveability, are significant factors in achieving an automotive engine with the potential for good performance and low exhaust emissions.

The purpose of the research work to be described in the following pages has been to develop a model to predict the performance of the TCCS stratified charge engine given the engine geometry, operating parameters and the fuel properties. Once the model is shown to be effective in predicting the performance it can then be used as a design tool. With the brief description of the geometry and the mode of operation of the engine given above, we will now proceed to a discussion of the model.

THE MODEL

BASIS FOR THE MODEL DEVELOPMENT - A set of performance data including pressure-volume diagrams was supplied by Texaco at the beginning of our research program. The data was obtained on an engine having a different geometry (a hemispherical combustion chamber rather than the cup-in-the-piston); however, the engine used the basic TCCS concept and it was felt that an analysis of this data would give some insight into the working of the engine. Data, for various speeds, loads and fuels, was plotted in the form of PV^{γ} plots. Because PV^{γ} is constant for an isentropic process and changes only due to real effects (which are small), an examination of the value of PV^{γ} just before, during and after combustion gives a very good idea of the net heat input or output to the working fluid due to heat release as a result of chemical reaction and/or heat losses.

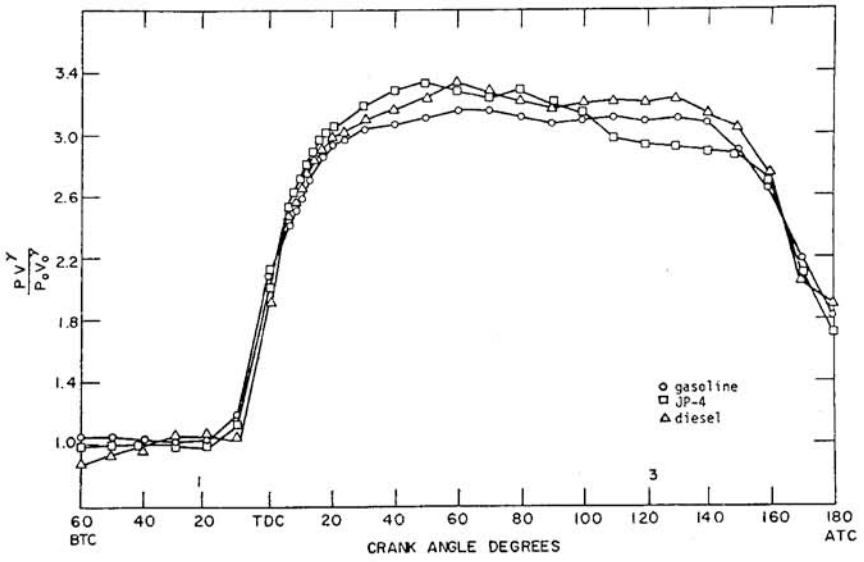

Fig.2 - PV^γ plot using experimental data on HCC engine—1200 rpm, full load

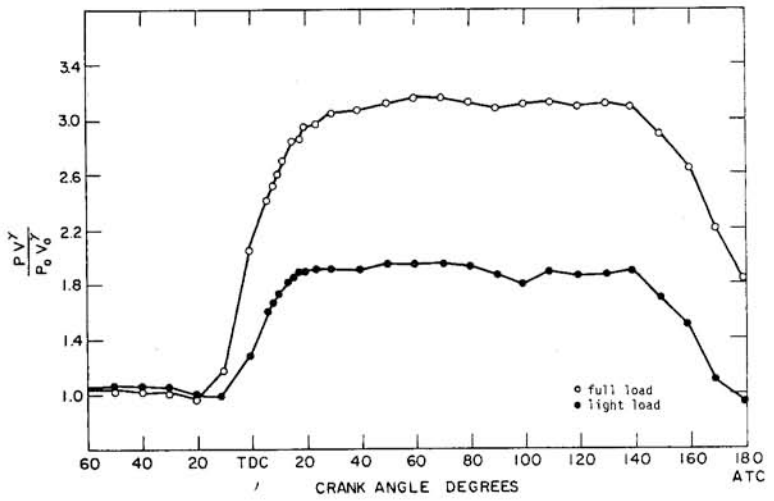

Fig.3 - PV plot using experimental data on HCC engine—1200 rpm, gasoline

Some typical PV^γ plots are shown in Figures 2 and 3. Figure 2 is for 1200 RPM full load case with three different fuels - gasoline, JP-4 and diesel and Figure 3 is set for 1200 RPM with two different load conditions with gasoline as the fuel. In generating these plots, the cylinder pressure and volume at start of injection have been used as the reference (P_o, V_o). The value of the specific heat ratio γ during and after combustion corresponds to that for burned gas mixtures at the overall equivalence ratio. While this will not be strictly correct - especially during combustion when γ changes from the value for unburned mixture to that of the burned gas mixture - the error introduced is small since combustion is rapid and takes place near top dead center. The ratio of volumes (V/V_o), thus, is close to one. Since the purpose of this analysis has been to obtain a qualitative understanding of the processes taking place, a slight error in the value of γ can be tolerated.

Some general conclusions can be drawn on the basis of this analysis. The steep rise in the value of PV^γ appears to correspond to the duration of injection. This suggests that the fuel burns as soon as it reaches the vicinity of the spark plug with an ignition delay that corresponds to the penetration time of the fuel jet from injector to spark plug. The lower

rates of increase in the value of PV^{γ} that follows this steep rise appears to be mixing controlled. The fact that PV^{γ} starts to drop later in the cycle suggests that as mixing nears completion, heat losses to the engine walls dominate. Another interesting conclusion is that there appears to be no substantial difference in the general nature of these plots for the different fuels considered here. It must be noted that the total chemical energy input, that is the mass injected times the lower heating value of the fuel, was also approximately the same for all three fuels.

In addition to the performance data, a high speed movie of the combustion process inside the engine cylinder was also supplied by Texaco. The combustion movie showed that first increments of the fuel to be injected took only a few crank-angle degrees to reach the spark plug and that these increments were ignited as soon as they reached the spark plug. This observation confirmed the conclusion derived from analyzing the PV^{γ} plots.

The information obtained from the analysis of the pressure-volume data, the combustion movie and from the literature on the development of the TCCS concept was used as the basis for a simplified theoretical model to predict the performance of the engine.

THE PERFORMANCE MODEL: QUALITATIVE DESCRIPTION - The model divides the complete engine cycle into the following phases: intake, compression, rapid combustion, mixing dominated expansion, heat transfer dominated expansion and exhaust. It assumes that rapid combustion follows the injection process with a time delay equal to the fuel transit time from injector to spark plug. The delay period is treated as part of the compression phase and the presence of the small quantities of injected fuel is neglected for the analysis. The rate of heat release during the rapid combustion phase is determined by the rate of fuel injection and the rate of entrainment of air by the fuel spray. Rapid combustion is assumed to occur at a fixed combustion equivalence ratio determined by an analysis of the process of spray formation and air entrainment. This analysis of the process of spray formation and entrainment of air by the fuel jet is treated by a jet mixing analysis. (Appendix I) Of course, in reality, combustion takes place at a wide range of equivalence ratios across the jet but for the purpose of performance modelling the net effective heat release rate can be assumed to take place at the mean equivalence ratio determined by the analysis mentioned above.

During the rapid combustion and the mixing dominated phases, the charge inside the cylinder will consist of a plume of hot burned gas surrounded by an unburned gas mixture. We observe from the combustion movies that the plume starts at the spark plug and is swept around by the air motion in the combustion chamber. Figure 4 qualitatively shows the initial stages of the hot burned gas plume. The sectional view shown in Figure 4 is taken through the cylinder axis and spark location. In the initial stages, the plume can be considered to be a section of a torus. As more and more fuel is injected and burned, the hot burned gas plume closes on itself forming a complete torus. The geometry of the plume is modified as it grows larger as discussed in Appendix II. Once the mixing process is complete, the charge inside the cylinder consists of burned gas alone and the plume occupies the total cylinder volume. Thus, during the rapid combustion and the mixing dominated phases, the total wall area for heat transfer can be divided into two parts - one in contact with the hot, burned gas plume and the other in contact with the relatively cold, unburned gas. The plume geometry model, described in Appendix II, is then used to obtain the two areas for heat transfer during these phases.

A better understanding of the various phases introduced in the model can be obtained by referring to PV^{γ} plots, as shown in Figure 5. Let us first consider a hypothetical case where there is no heat transfer to or from the working fluid and where intake and exhaust processes have not been included. In this case, the value of PV^{γ} remains constant during compression and fuel injection begins near the end of the compression phase.

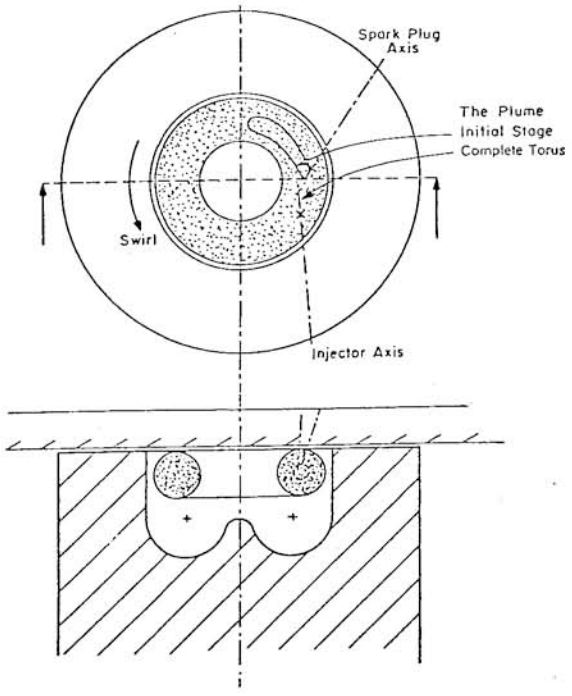

Fig.4 - Initial stages of the hot burned gas plume

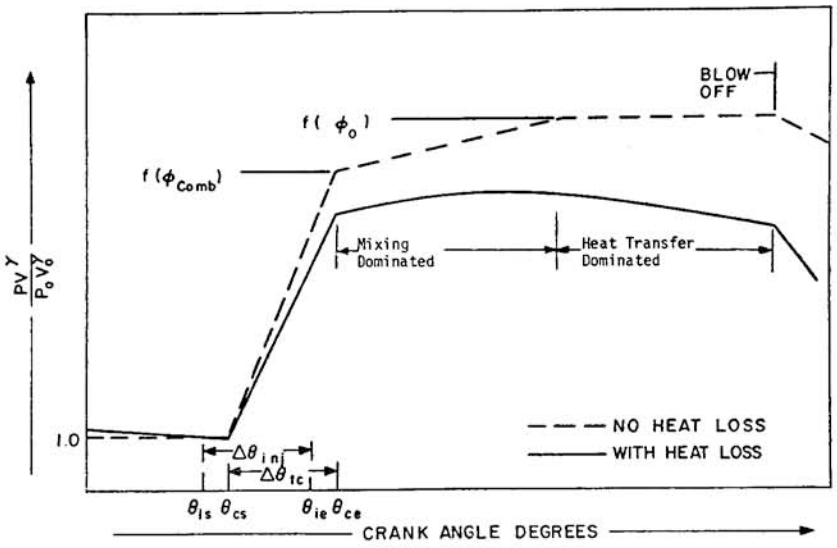

Fig.5 - Simplified PV^γ plot (theory). $\Delta\theta i_{nj}$ and $\Delta\theta_{rc}$ are injection and rapid combustion durations respectively

The delay period, before the start of the rapid combustion, is treated as part of the compression phase and the presence of small quantities of fuel is ignored. During the rapid combustion phase, the value of PV^γ rises rapidly and the rate of rise is determined by mass rate of injection and the assumed combustion equivalence ratio. At this point in the cycle, we have a plume of hot burned gas surrounded by relatively cold air. As the plume entrains surrounding air, additional chemical heat release and/or the mixing of hot and cold gases with different heat capacities results in an additional rise in the value of PV^γ. This is the mixing dominated part of the expansion phase and it ends when all of the air is "consumed" by the hot burned gas plume. Now the whole charge consists of the burned gas at the overall fuel-air ratio for the cycle and as we have assumed no heat transfer to or from the working fluid, the value of PV^γ remains constant until the exhaust valve opens. The effect of heat transfer can now be put in qualitatively - a heat loss from the working fluid lowers the value of PV^γ as shown by the solid curve in Figure 5. With this qualitative description of the various phases, we now proceed to a detailed, quantitative treatment of each of the phases and, thereby, of the complete cycle.

THE PERFORMANCE MODEL: QUANTITATIVE DESCRIPTION - Before giving a description of the individual phases, we will discuss some aspects of the model which are common for all phases. These include treatment of gas properties (both unburned and burned gas) and the treatment of heat transfer in general.

Gas Properties - For air, heat capacities have been treated as functions of temperature alone. The burned gas properties have been treated on the basis of some approximate relationships developed by Michael K. Martin (6) at the Sloan Automotive Laboratory. These approximate relationships have been checked against a thermodynamic equilibrium program involving some 46 different species with agreement to $\pm$ 3% over the range of interest.

Heat Transfer Correlation - Heat transfer has been treated largely with a technique based on Woschni's universal correlation (7). The gas velocities have been modified to include the effect of high swirl which is assumed to be additive. The swirl is treated as solid body rotation near top dead center where most of the events of interest occur and the velocities due to swirl dominate. Heat transfer areas are divided into two parts and the heat transfer coefficient for each part is calculated separately. The total heat transfer is obtained by adding the contributions of each of the parts (see Appendix II).

We will now begin with a detailed description of the compression phase. Assumptions for each of the phases will be explicitly noted and the equations used for predicting pressure and other performance parameters will be described. The gas properties and the heat transfer are treated as noted above.

Compression Phase - During the compression phase, the charge is considered to be a homogeneous mixture of air, residual gas and the exhaust gas recirculated (EGR). This mixture will from now on, be referred to as the "unburned gas mixture". As stated earlier, the presence of the small quantity of fuel during

the ignition delay period will be neglected. With these assumptions, we can write down the equation of state and mass and energy conservation equations as follows:

Equation of state

$$PV = m_u R_u T \tag{1}$$

Mass conservation

$$m_u = (m_u)_o \text{ or } v_u = \frac{V}{m_u}$$

Energy conservation

$$E-W-Q = m_u e_u \tag{2}$$

where work done $W = \int PdV$, and,

$$(m_u)_o = (m_A)_o + m_{RG} + m_{EGR}$$

The subscript 'u' refers to unburned gas and $(m_A)_o$, m_{EGR} are the masses of air, residual gas and recirculated exhaust gas at the end of intake stroke. The recirculated and residual exhaust gas fractions are defined as follows:

$$EGR = m_{EGR}/[(m_A)_o + m_{EGR}] \tag{4}$$

$$RG = m_{RG}/[(m_A)_o + m_{EGR} + m_{RG}] \tag{5}$$

so that

$$m_{EGR} = (EGR)*(m_A)_o/(1-EGR) \tag{6}$$

$$m_{RG} = (RG)*[(m_A)_o + m_{EGR}]/(1-RG) \tag{7}$$

It is assumed that residual gas and the recirculated exhaust gas are burned gases at the overall equivalence ratio. Gas properties for the burned gases and air as well as the heat transfer (Q) are obtained from the analyses described in previous section of this paper. Equations (3), (6), and (7) with gas properties are used to determine the right-hand side of Equation (2) and these equations can be used to predict the pressure. As both W and Q involve pressure (P) and/or temperature (T) in their evaluation, a simple iterative scheme is used.

Rapid Combustion Phase - The rapid combustion phase is assumed to follow fuel injection after the jet transit time delay. As previously described we assume that rapid combustion takes place at a constant combustion equivalence ratio for the purpose of performance modelling. The unburned gas entrained by the fuel when it reaches the spark plug is known from the spray analysis (Appendix I) and the combustion equivalence ratio (ϕ_c) can be determined as follows: Let the ratio of the mass of unburned gas entrained to the mass of fuel at the spark plug be $(G-F)_{sp}$. The fraction of air in a unit of mass of unburned gas mixture is:

$$\frac{(m_A)_o}{(m_u)_o} \tag{8}$$

The combustion equivalence ratio (ϕ_c) then is:

$$\phi_c = \frac{(m_u)_o}{(m_A)_o * (G-F)_{s/p} * F_c} \tag{9}$$

where F_c is the chemically correct fuel-air ratio. Because the gas mixture entrained in the burned gas plume contains residual gas, and air, the equivalence ratio of the hot burned gas plume is different than ϕ_c. This equivalence ratio ϕ can be calculated if it is assumed that the residual gas and the exhaust gas recirculated are burned gases at the overall equivalence ratio ϕ_o.

The charge inside the cylinder can then be considered as consisting of a plume of hot burned gas at the equivalence ratio, ϕ, and the unburned gas mixture outside the plume. The equations of state and mass and energy conservation can then be written as follows:

Equations of state

Unburned gas mixture

$$PV_u = m_u R_u T_u \tag{10}$$

Burned gas

$$PV_b = m_b R_b T_b \tag{11}$$

Mass conservation:

$$m_u + m_b = (m_u)_o \tag{11}$$

Energy conservation:

$$E-W-Q = m_u e_u + m_b e_b \tag{12}$$

Also, note that $V_u + V_b = V$

The work (W) heat transfer (Q) and gas properties are treated as described earlier. Of course, the heat transfer now must be divided into two parts due to the presence of the hot, burned gas plume.

These equations have again been solved using a simple, iterative scheme to predict cylinder pressure and other performance parameters as a function of time (crank-angle degrees) during the rapid combustion phase. The rapid combustion phase ends when all the injected fuel has reached the spark plug.

Expansion Phase - This phase starts at the end of the rapid combustion phase and continues until the exhaust valve starts to open when blowdown and the exhaust phase take over. This phase bas been divided into two parts, a mixing dominated phase and a heat transfer dominated phase.

(a) Mixing Dominated Expansion Phase - At the beginning of this phase, the charge

inside the cylinder is considered to consist of a hot, burned gas plume surrounded by a relatively cold unburned gas mixture. The plume slowly entrains this surrounding gas and as it does so, it is assumed that the entrained gas is perfectly mixed throughout the plume resulting in a new equivalence ratio for the plume at any instant. This entrainment and mixing also results in some chemical heat release due to combustion if the plume is initially richer than stoichiometric.

The entrainment of the surrounding gas mixture by the plume has been treated following the work of Blizard and Keck which relates the turbulent eddy entrainment velocity to the engine inlet speed. The surface area of the plume for entrainment of the surrounding gas mixture is obtained from the plume geometry model (Appendix II). Thus the mass rate of entrainment of surrounding gas mixture can be given as

$$\dot{m} = S_e U_e \sqrt{\rho_u \rho_b} \qquad (13)$$

Where the plume area S_e at any instant is given by the plume geometry model and the turbulent eddy entrainment velocity, U_e, is taken from Blizard and Keck:

$$U_e \simeq 0.28\ U_i$$

and

$$U_i = \varepsilon_v (b^2/2DL)NS \qquad (14)$$

Knowing the mass rate of entrainment, the fractions of the constituents of the entrained gas mixture and the old equivalence ratio of the plume; the new equivalence ratio for the plume is calculated. Thus the charge in the cylinder during this phase can be treated exactly like that during the rapid combustion phase except that the equivalence ratio of the plume now changes, in contrast to a constant combustion equivalence ratio during the entire rapid combustion phase. The varying equivalence ratio is taken into consideration when evaluating the plume gas properties. Since the rest of the treatment is exactly similar to that during the rapid combustion phase, the equations of state and mass and energy conservation will not be repeated here.

The mixing dominated phase persists until all of the unburned gas mixture has been entrained, or, if mixing is not complete, until the exhaust valve starts to open. In the latter case, there is no heat transfer dominated phase and at the start of blowdown, the mixing dominated phase is terminated. The composition is frozen and mean gas properties overall are defined. If, on the other hand, mixing is complete before the exhaust valve starts to open, it is followed by the heat transfer-dominated phase.

Heat Transfer Dominated Expansion Phase - At the beginning of this phase, the charge inside the cylinder is considered to be homogeneous burned gas at the overall equivalence ratio as the mixing is now complete. The treatment, then, is similar to that for the compression phase except that the charge is burned rather than unburned gas. The only important process going on is the heat transfer to the walls. The equations, replacing subscript 'u' by subscript 'b' for those of the compression phase are

Equation of state:

$$PV = m_b R_b T$$

Mass conservation:

$$m_b = (m_u)_o \text{ or } v_b = \frac{V}{m_b}$$

Energy conservation:

$$E-W-Q = m_b e_b$$

and the performance is predicted in a manner similar to that in the compression phase. This phase ends when the exhaust valve starts to open.

Exhaust and Intake Phases - The mass flow rates through exhaust and intake valves have been treated as quasi-steady flow through a restriction. The governing equations can be written as follows:

$$\dot{m} = C_v A_v \left(\frac{RT_o}{P_o}\right) (\gamma RT_o)^{1/2} \{(2/(\gamma-1)) \left[\left(\frac{P_2}{P_o}\right)^{2/\gamma} - \left(\frac{P_2}{P_o}\right)^{(\gamma+1)/2(\gamma-1)}\right]\}^{1/2} \qquad (15)$$

for subsonic flow, and

$$\dot{m} = C_v A_v \left(\frac{P_{oc}}{RT_{oc}}\right) (\gamma RT_o)^{1/2} \left\{\left[\frac{2}{(\gamma+1)}\right]^{(\gamma+1)/2(\gamma-1)}\right\}^{1/2} \qquad (16)$$

for choked flow, with the condition for choked flow being:

$$\frac{P_o}{P_s} > \left(\frac{\gamma+1}{2}\right)^{\gamma/(\gamma-1)} \qquad (17)$$

where C_v = valve discharge coefficient

A_v = valve flow area

P_o, T_o are upstream stagnation pressure and temperature

P_2 = downstream static pressure and P_{oc}, T_{oc} are stagnation pressure and temperature for choked flow. The flow through exhaust and intake valves is treated with these equations and the logic to take care of the reverse flows through the valves has been included in the computer program. Before these equations can be used to obtain the mass rates of flow, a knowledge of discharge coefficients and valve flow areas is required both for exhaust and intake valves. This information has been obtained from the data supplied by Texaco.

In addition to the flow equations, equations of state, mass and energy conservation are used to model the exhaust and the intake phases. The equations of state and mass conservation are:

$$PV = mRT \tag{18a}$$

$$m = (m_u)_o + m_{in} - m_{ex} \tag{18b}$$

The energy equation for an open system, after some mathematical manipulation and use of equation of state, can be written as follows

$$\frac{\dot{T}}{T} = \frac{R}{C_p - R}\left[\frac{(\dot{m}_{in} h_{in} - \dot{m}_{ex} h_{ex} - \dot{m}h) - \dot{Q}}{mRT} - \frac{\dot{MW}}{MW} + \frac{\dot{V}}{V} - \frac{\dot{m}}{m}\right] \tag{19}$$

The energy equation (19) along with the flow equations (16 or 17) and the equations for heat transfer and work form a set of simultaneous linear differential equations. These have been solved numerically using a fourth order Runga-Kutta method resulting in the predictions for the exhaust and intake phases.

Thus the performance modelling of the cycle is complete. In addition to the detailed performance predictions made during each of the phases, the overall engine performance parameters can also be obtained. The predictions for the motored engine can also be obtained from the complete model by removing rapid combustion and mixing dominated phases leaving the intake, compression, expansion, and exhaust phases.

A number of computer programs have been developed to carry out the steps described in the model and give as outputs, overall performance, detailed performance and plots of cylinder pressure and PV^{γ} as functions of crank-angle.

The model, as described, requires an input from the spray analysis; specifically, the entrained gas to fuel ratio at the spark plug. In addition, we have not explicitly discussed the multi-fuel capability of the engine and have not indicated the limitations of the model as with regard to type of fuels for which the model can be used. These questions appear to be more properly addressed in the spray analysis in Appendix I.

PREDICTIONS OF THE MODEL

COMPARISON WITH EXPERIMENTAL DATA - A 3 7/8" x 3 7/8" single cylinder engine designed by Texaco has been set up at the Sloan Automotive Laboratory at MIT to carry out experimental investigations on the TCCS Stratified charge concept. A CFR 48 crankcase has been modified to accept a cylinder sleeve assembly, head, crankshaft, piston and valve train assembly supplied by Texaco.

In addition to the preliminary data obtained with the single cylinder engine set up at the Sloan Automotive Laboratory, similar data has been supplied by Texaco. The performance model has been used in conjunction with the gas-to-fuel ratio supplied by the jet model to predict engine performance starting from the engine geometry, operating conditions and fuel properties. The predictions have then been compared with the available engine data from Texaco as shown in Figures (6) and (7). The fuel used at Texaco was gasoline and injection timing was set at 28° BTC for 2500 RPM and at 20° BTC for 1500 RPM at full loads. As shown in Figures (6) and (7) the predictions of the model agreed well with the experimental data obtained from single cylinder engine set ups.

The performance model can also be used in conjunction with the performance of the engine if any of the input parameters are changed. The models, therefore, have a potential to be used as design tools.

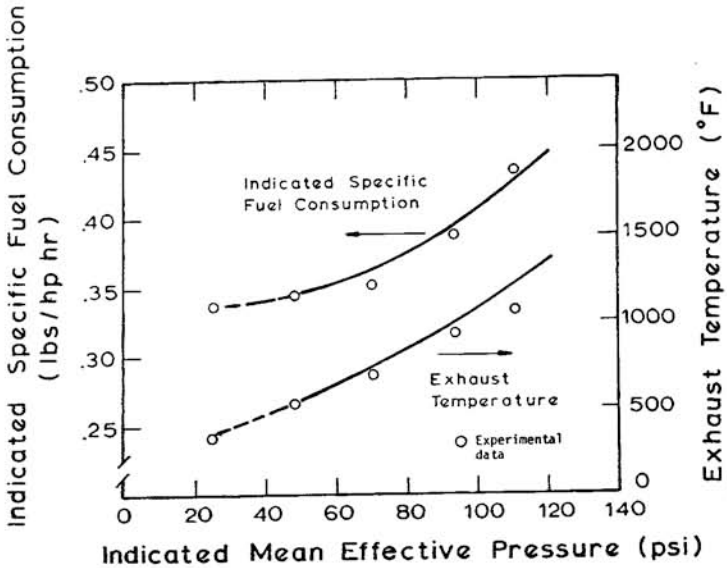

Fig.6 - Predictions of the model compared with experimental data-1500 rpm

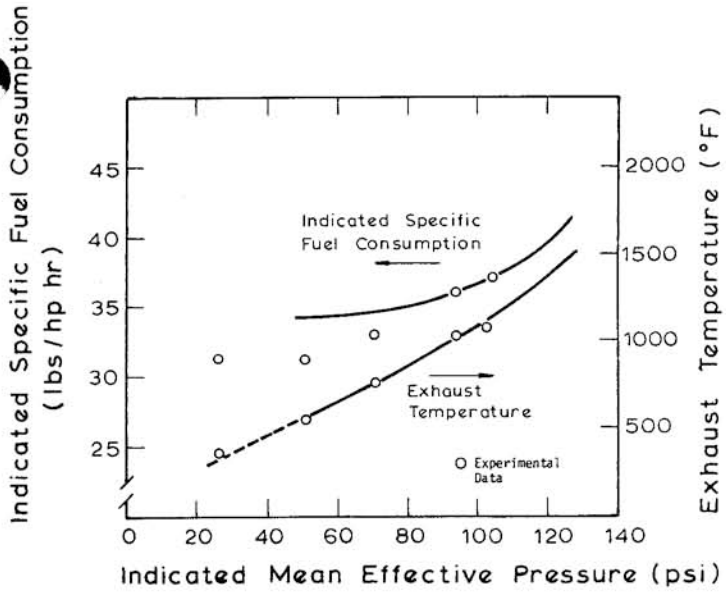

Fig.7 - Predictions of the model compared with experimental data-2500 rpm

PREDICTIONS OF THE PERFORMANCE MODEL AND ITS USES AS A DESIGN TOOL - A parametric study has been carried out with the performance model to demonstrate this potential as a design tool. The various parameters considered are the fraction of the exhaust gas recirculated (EGR),injection timing, gas-to-fuel ratio at the spark plug and the duration of injection. The calculations have been carried out for 2500 RPM engine speed and of 3/4 of the full load fuel injection. All parameters are held at their present design values except the single parameter to be considered. The present design values as well as the range of parameters used in this study have been listed in Table 1.

The effects of these changes on performance as predicted by the model are shown in Figures (8) through (12). In these figures the top box shows the next work done, heat loss and the energy of the exhaust gas as a fraction of the total chemical energy of the injected fuel. Below it are the indicated mean effective pressure and the blowdown temperature defined as the temperature of the exhaust gas at the beginning of blowdown. Because the amount of total fuel injected is fixed for all the cases to be described, the curve for indicated mean effective pressure is also a measure of the inverse indicated specific fuel consumption. A dotted vertical line shows the present design and operating conditions in all figures.

Figure (8) shows the effect of various fractions of EGR on the performance as predicted by the performance model. As the exhaust gas recirculated increases, the indicated mean effective pressure and thereby the power output goes down. Looking at the energy balance we see that the heat loss also goes down whereas the energy of the exhaust gases increases to compensate for the other two. Of course, because of the excess air operation of the engine for part loads, the loss in power output is not quite as dramatic as it would be at full load where any amount of EGR will result in a reduction in the amount of air available for combustion.

The effect of changing the start of in-

Table 1 - List of Inputs for Parametric Analysis Using the Performance Model

Present values of the parameters at 2500 RPM, 45 mm^3 Fuel/Injection.

% Exhaust gas recirculated	= 0.
Injection timing (start)	= 25°BTC
Gas-to-fuel ratio	= 10.6
Injection duration	≃ 32 CA°

Range of Values for Parametric Study

Parameter	
% Exhaust gas recirculated	0, 5,10,15,20
Injection timing, °BTC	45'35,25,15, 5
Gas-to-fuel ratio at the spark plug	6, 8,10.6,13,16
Injection duration, CA°	10,20,30,40,50

[A square wave injection profile is assumed]

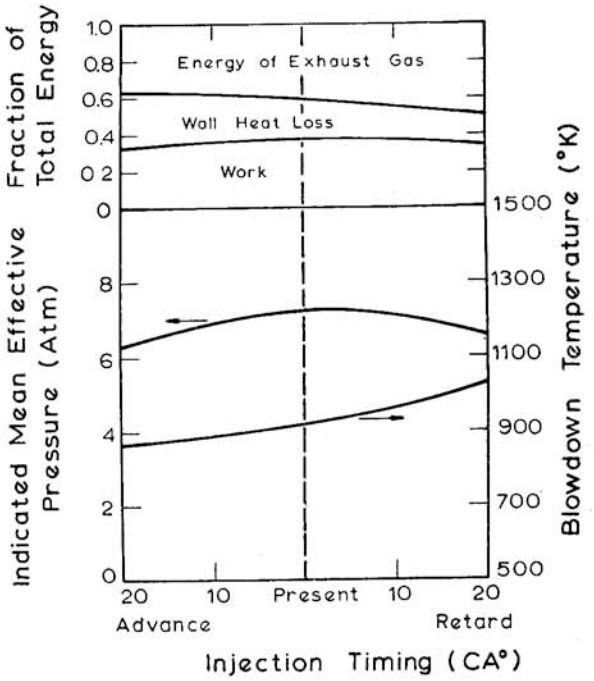

Fig.8 - Effect of exhaust gas recirculated on engine performance

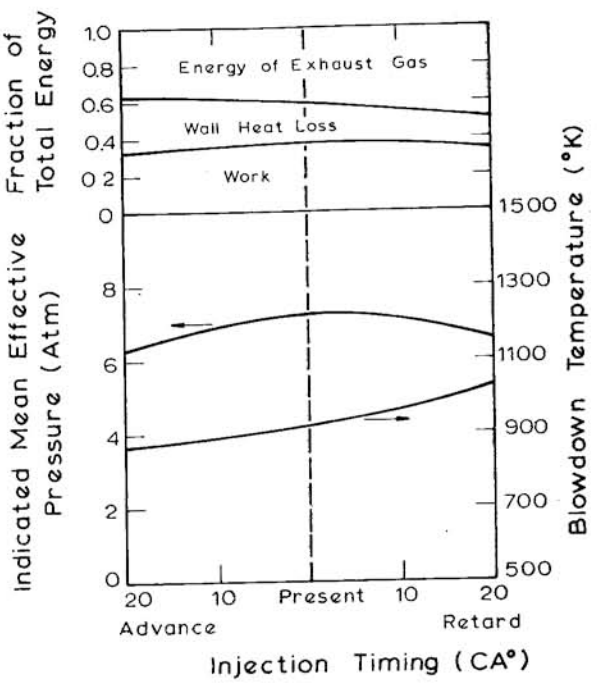

Fig.9 - Effect of injection timing on engine performance

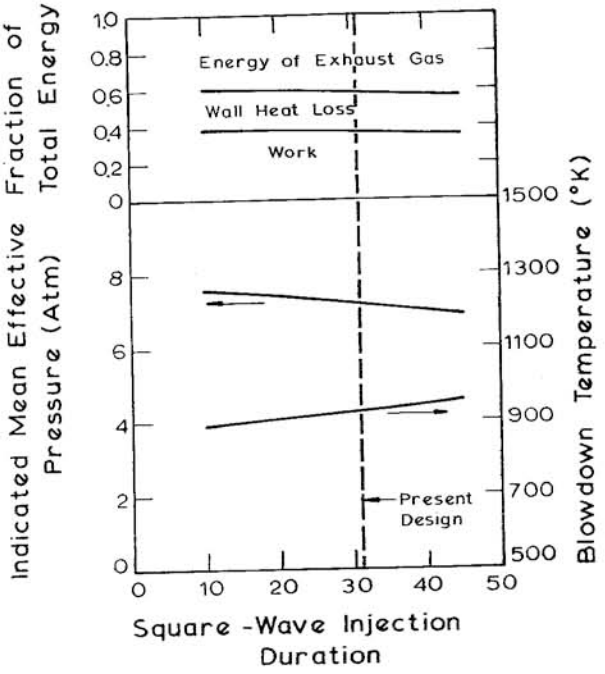

Fig.11 - Effect of injection duration engine performance

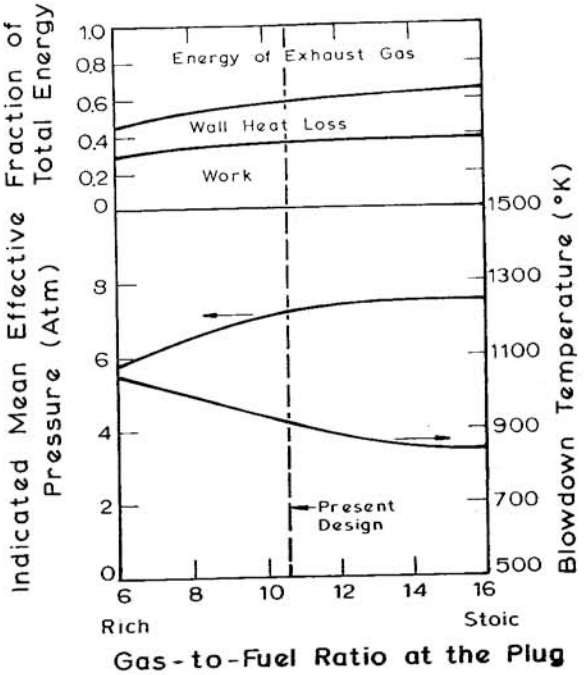

Fig.10 - Effect of gas-to-fuel ratio on engine performance

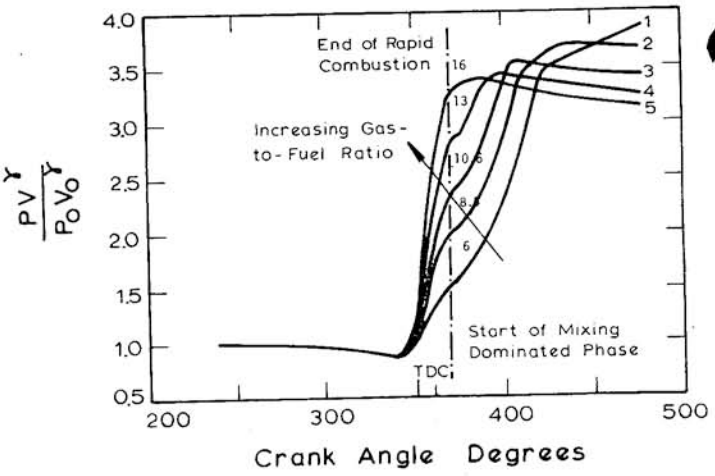

Fig.12 - Effect of gas-to-fuel ratio at the plug on PV^{γ}

jection is shown in Figure (9). As far as the power output and fuel consumption are concerned, the present timing is very close to optimal as expected from performance data. Both advancing as well as retarding the injection from its present value adversely affect the power output. As can also be seen from the figure, the energy of the exhaust as well as the blowdown temperature rise as injection is retarded. The peak pressure in the cycle is found to vary from 30 atmospheres to almost 60 atmospheres as the injection timing is advanced.

Figure (10) shows the effect of a change in the gas-to-fuel ratio at the spark plug. There are many ways in which this ratio can be changed by changing injection parameters. While the other two parameters discussed so

far - EGR and the injection timing can be classified as operating conditions easily amenable to change, a change in the gas-to-fuel ratio at the spark plug requires basic design changes - a change in the distance between nozzle tip and the spark plug, modified swirl rates or a change in the injection system such as orifice size or angle of injection. As can be seen from Figure (10), any reduction in gas-to-fuel ratio from the present value will adversely affect the performance. This is to be expected because a lower gas-to-fuel ratio means that less of the total chemical energy is released during "rapid combustion" and more is released during the slower, mixing-dominated phase of the expansion stroke. As the gas-to-fuel ratio is farther reduced, the mixing may not be complete as the exhaust valve opens. When more chemical energy is released later in the expansion phase, the energy in the exhaust and its temperature will rise. An increase in gas-to-fuel ratio at the plug, on the other hand, increases the power output - but only marginally and as we reach stoichiometric mixtures at the spark plug, the indicated mean effective pressure curve flattens out. Considering that the gain in performance is only marginal if the ratio is increased, any design changes to bring about this increase would have to be carefully scrutinized. There may be some considerations - other than the power output - which may weigh in favor of a less rich or even slightly lean rapid combustion phase; including reduction in soot and oxides of nitrogen. The peak pressures in the cycle rise to nearly 63 atmospheres as the rapid combustion approaches stoichiometric gas-to-fuel ratios.

Figure (12) shows a typical set of PV^{γ} plots obtained from a parametric study of gas-to-fuel ratio. These plots very clearly show that as the gas-to-fuel ratio at the spark plug is increased, more heat is released during the combustion phase.

The last parameter considered here is the duration of injection as shown in Figure 11. The injection is assumed to be a square wave pulse. The injection timing is assumed to be such that the start and end of the rapid combustion are symmetrical about top dead center. As we see from the figure, there is a small gain in the power output as the injection duration is reduced. Of course, the rate rates of pressure rise go higher as the duration is reduced - cylinder pressure rising from 22 to 55 atmospheres in 10 crank-angle degrees for the extreme case considered here.

Clearly, these are but a few examples where the model can be used to predict the effect of proposed changes in the design and/or operating conditions of the engine on engine performance. The purpose here has been to bring out the potential application of the model as a design tool rather than to provide an exhaustive mapping of all possible changes.

CONCLUSIONS AND DISCUSSIONS

(i) A performance model for the Texaco Controlled Combustion, Stratified Charge Engine has been developed to predict engine performance starting from engine geometry, fuel characteristics and the operating conditions.

(ii) Parametric analysis has been carried out using the performance model to illustrate its potential use as a design tool.

(iii) This preliminary model shows good agreement between predicted and measured engine performance. In particular, the use of a jet model in setting the initial conditions for the problem introduce considerable design capability. However, a complete model should include emissions and our current work is directed toward extending our preliminary model in this direction.

REFERENCES

1. Davis et al., "Fuel Injection and Positive Ignition - A basis for Improved Efficiency and Economy," Paper 190A presented at SAE Summer Meeting, Chicago, June, 1960.

2. Mitchell, et al., "Design and Evaluation of a Stratified Charge Multifuel Military Engine," SAE Transactions, Vol. 77 (1968), Paper 680042.

3. Mitchell et al., "A Stratified Charge Multifuel Military Engine - A Progress Report," SAE Paper 720051.

4. Alperstein, et al., "Texaco's Stratified Charge Engine-Multifuel, Efficient, Clean and Practical," SAE Paper 740563.

5. R.E. Canup, "The Texaco Ignition System - A New Concept for Automotive Engine," SAE Paper 750347.

6. M.K. Martin, "Photographic Study of Stratified Combustion Using a Rapid Compression Machine," S.M. Thesis, M.I.T., 1975.

7. G. Woschni, "A Universally Applicable Equation for the Instantaneous Heat Transfer Coefficient in the Internal Combustion Engine," SAE Paper 670931.

8. N. Blizard and J.C. Keck, "Experimental and Theoretical Investigation of Turbulent Burning Model for Internal Combustion Engines," SAE Paper 740191.

9. M. Lazarewicz, "Performance of Texaco Stratified Charge Engine on Gasoline," S.M. Thesis, M.I.T., 1975.

LIST OF SYMBOLS

The following symbols have been used throughout the text unless otherwise noted.

A_a	Wall area in contact with the hot burned gas mixture
A_b	Wall area in contact with the hot burned gas plume
A_{cup}	Surface area of the cup in the piston
A_T	Total wall area for heat transfer
b	Cylinder bore
C_p	Specific Heat at constant pressure
C_V	Specific heat at constant volume
D	Effective valve diameter
d_c	Diameter of the cup in piston
E	Total internal energy
e	Specific internal energy
F_c	Chemically correct fuel to air ratio
$(G-F)_{S-P}$	Gas-to-fuel ratio at the spark plug
h	Specific enthalpy
L	Valve lift
LHV	Lower heating value of the fuel
m	Mass in the cylinder
m_{ex}	Cumulative mass flow through exhaust valve during exhaust phase
m_{f_b}	Mass of fuel burned
m_{in}	Cumulative mass flow through intake valve during intake exhaust
MW	Molecular weight
$\dot{m}$	Mass rate of flow
$\dot{m}_e$	Mass rate of entrainment by the plume
N	Engine speed
P	Cylinder pressure
Q	Heat transfer to the walls
R	Specific gas constant
r	Characteristic plume radiums
S	Stroke of the engine
S_e	Surface area of the plume for entrainment
T	Temperature
U_e	Eddy entrainment velocity
V	Total volume
v	Specific volume
V_{cup}	Volume of the cup in the piston
V_s	Swirl velocity
W	Work done by the charge
γ	Ratio of the specific heats
ρ	Density
ϕ	Equivalence ratio
ϕ_c	Equivalence ratio for combustion during rapid combustion phase
ϕ_o	Overall equivalence ratio

Subscripts

A	Air
b	Burned gas
cup	Cup in the piston
EGR	Exhaust gas recirculated
e	Entrainment
ex	Exhaust
i	Inlet
in	Intake
O	Reference-at the end of intake phase or beginning of compression phase
RG	Residual gas
u	Unburned gas mixture
v	Volumetric
w	Engine walls

ACKNOWLEDGEMENT

The authors are thankful to Professors Heywood and Hoult of M.I.T., Mr. Ed Mayer of Texaco and Mr. Walter Bryzik of USATACOM for their help in this work. Technical and financial support for this research was provided by U.S. Army-Tank Automotive Command by subcontract to M.I.T. from Texaco, Inc., under contracts No. DAAE07-73-C-0282, DAAE07-74-C-0268, and DAAE07-74-C-0168.

APPENDIX I

FUEL-AIR MIXING IN THE TEXACO CONTROLLED COMBUSTION STRATIFIED CHARGE ENGINE

The purpose of the research work described in the following pages has been to carry out a spray analysis as part of the general effort to develop a model to predict the performance of the Texaco Controlled Combustion System (TCCS) stratified charge engine; given engine geometry, operating parameters and the fuel properties. The analysis begins with the assumption that the process of the spray formation in engines can be studied using continuum models. Such an approach has been used earlier by Rife and Heywood (A2) in studies of diesel combustion in a rapid compression machine; and they conclude that the motion of the fuel jet can be satisfactorily analyzed with such models. As reported by Rife and Heywood (A2), this approach assumes that the fuel breaks into droplets near the nozzle orifice and that the relative velocity of droplets in the jet flow is small. They have also concluded that special entrainment assumptions are not required for modelling the fuel jet in an engine; so that standard entrainment coefficients can be used.

Characteristic Length Analysis - A schematic of the spray and various characteristic lengths for the TCCS engine and the fuel spray are shown in Figure AI-1. The important characteristic lengths are:

(i) Distance between nozzle-tip and spark plug plane L_{sp}

(ii) Jet break-up length L_b

(iii) Droplet deceleration length L_{ev}

(iv) Momentum length L_{mom}

As suggested previously, our combustion model is applicable if most of the fuel is evaporated by the time it reaches the spark plug plane. For continuum jet models to apply we required:

(a) Rapid jet break-up and droplet deceleration occuring within a few orifice diameters or "at the nozzle tip".

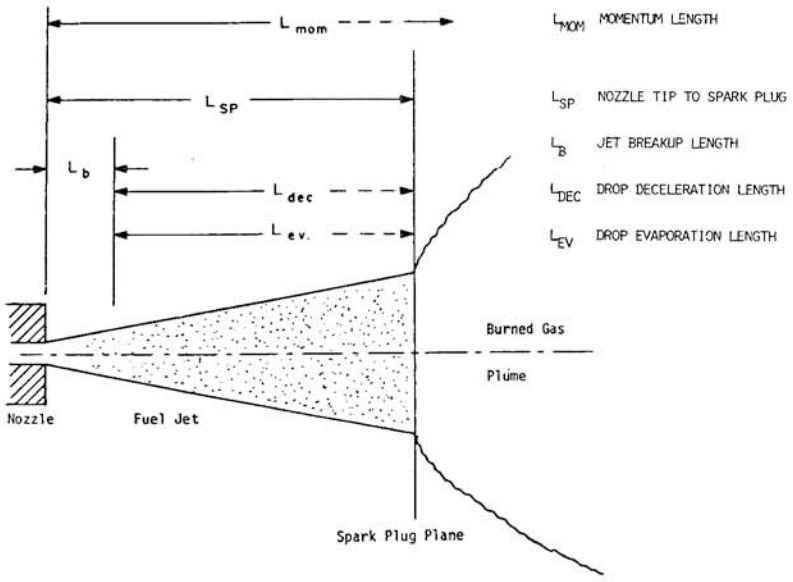

Fig.A1-1 - Spray schematic and characteristic lengths

$L_b, L_{dec} \ll L_{sp}$

(b) Most of the fuel must be evaporated by the time it reaches the spark plug.

$L_{ev} \simeq L_{sp}$

The momentum length L_{mom} defines the length scale over which the momentum introduced into the jet by entrainment of the cross flow is equal to the initial momentum of the jet. The momentum length determines the relative bending of the jet centerline. If $L_{mom} \ll L_{sp}$, we can neglect the bending of the jet centerline due to cross flow; otherwise, the effects of cross flow must be included in studying the space-time history of the jet.

Jet Break-up - It is generally recognized that there are several different modes of jet break-up depending upon the velocity of the fluid jet. Four modes were identified by Haenlein (A7) including "complete and immediate disruption of the jet". Other modes were analyzed mathematically by Weber (A8) but there is no treatment by either Haenlein or Weber of this mode. A similar definition of atomization modes was stated by Ohnesorge (A9) along with empirically defined dimensionless numbers to predict the boundaries between the different modes. He defines the mode boundaries by relating a number Z characteristic of the fluid to the Reynolds number Re

where

$$Z = \eta/(\sigma\rho_f d)^{1/2} \qquad (A1\text{-}1)$$

and for mode boundaries

$$Z = Z(Re)$$

and η = absolute viscosity of the fluid

σ = surface tension of the fluid

ρ_f = liquid density

d = nozzle diameter

A simple dimensional analysis of the important forces (neglecting gravity) will show that the two relevant dimensionless numbers are the Weber number $We = \rho V^2 d/\sigma$ and the Reynolds number $Re = \rho V d/\eta$. The characteristic number Z can be formed for these two dimensionless groups by eliminating velocity. The minimum Reynolds number for immediate disruption is then given by Ohnesorge in terms of a power law

$$Z = c(Re)^n \qquad (A1\text{-}2)$$

where

$n = -1.26$

$c = 1096$

So that for immediate and complete break-up (i.e. $L_b \ll L_{sp}$):

$$Re \geq 259/Z^{.018} \qquad (A1\text{-}3)$$

This correlation is based on dimensional analysis and has been verified by Burt and Troth(A10). The characteristic number Z can be calculated given fluid properties and the nozzle orifice size. Substituting this into Equation (A1-3); we can establish the minimum Re for immediate disruption of the jet for the given fluid.

Deceleration of Droplets - Equating the change in momentum of the droplet to the aerodynamic drag force, we can give the characteristic deceleration time as:

$$\tau_{dec} \simeq D_{drop}\,(\rho_f/\rho_a)/C_D\,V_{initial} \qquad (A1\text{-}4)$$

where D_{drop} = droplet diameter
ρ_f = fluid density
ρ_a = air density
C_D = coefficient of drag
$V_{initial}$ = initial velocity of the droplet relative to air

The corresponding deceleration length then is

$$L_{dec} = \tau_{dec} \times V_{initial} = D_{drop} (\rho_f/\rho_a)/C_D \qquad (A1\text{-}5)$$

and for the model to be applicable

$$L_{dec} << L_{SP}$$

Droplet Vaporization - Based on Beer and Chigier(A11), the characteristic vaporization time can be given as

$$\tau_{ev} \simeq D^2_{drop}/\lambda \qquad (A1\text{-}6)$$

where λ is the evaporation is constant.

For a single stagnant drop in an infinite atmosphere, the evaporation constant λ_s is given as:

$$\lambda_s = 8\ k\ ln\ (1+b)/\rho_f C \qquad (A1\text{-}7)$$

where B = C(Tg-Ts)/Q = Transfer number
Q = latent heat of vaporization and sensible heat to raine droplet temperature to boiling point
Tg = mean gas temperature
Ts = droplet surface temperature
ρ_f = density of the fuel
C = specific heat of air
and k = thermal conductivity of air

A number of phenomena excluded by the assumption of a "single" stagnant drop in an infinite atmosphere can modify the evaporation rate of a droplet and the most important is the forced convective motion of the gas relative to the droplet. The effect of this phenomenon is included on the basis of a correlation given by Ranz and Marshall (A12) for Reynolds number between 0 and 200 and low values of B

$$\lambda = \lambda_s(1 + 0.30\ Sc^{1/3}\ Re^{1/2}) \qquad (A1\text{-}8)$$

where Sc = Schmidt number of the gas (equal to the ratio of momentum transfer to the mass transfer)

$$Sc = \mu_\infty/\rho_\infty D \qquad (A1\text{-}9)$$

and the Reynolds number (Re) is

$$Re = \rho_\infty U_\infty D_{drop}/\mu_\infty \qquad A1\text{-}10)$$

where ρ_∞ and μ_∞ are the density and viscosity of the gas far upstream from the droplet; D is the diffusion coefficient and U_∞ is the gas velocity relative to the droplet. In our case, for droplets of about ten micron size, the above correlation gives $(\lambda_i/\lambda_s) \sim 10\text{-}11$ where λ_i is based on the initial jet velocity. Since the actual case is somewhere in between and we will take

$$\lambda = (\lambda_i+\lambda_s)/2 \simeq 6\lambda_s \qquad (A1\text{-}11)$$

Equations (A1-6), (A1-7), and (A1-11) with the knowledge of mean droplet diameters can be used to calculate a characteristic length of vaporization. We will require that it be less than or comparable to the distance between nozzle tip and spark location so that almost all of the fuel is vaporized by the time it reaches the spark plug.

$$L_{ev} \leq L_{SP}$$

Momentum Length Considerations - The momentum length defines the length scale over which the sum of the momentum flux of the cross-flow across the jet boundary becomes equal to the initial momentum of the jet. This will determine whether the bending of the spray axis must be included in the analysis. From Hoult and Weil (A3) and Escudier (A5) the momentum length is:

$$L_{mom} = [\rho_o u_o^2 b_o^2/\rho_\infty V^2]^{1/2} \qquad (A1\text{-}12)$$

where ρ_o = initial density of the liquid jet
u_o = initial velocity of the jet
b_o = initial radius of the jet
ρ_∞ = density of the cross-flow
V = velocity of the cross-flow

The relationships between the characteristic lengths, fuel properties and injection system parameters have been established and the various characteristic lengths have been calculated for a wide range of fuels. These characteristic lengths have then been compared with the distance between nozzle-tip and the spark plug to ascertain the relationships required for our simple performance model. The types of fuels considered include methanol, gasoline diesel and a wide-range distillate. The physical properties of these fuels used in the calculations have been listed in Table A1-1 and the results of the calculations, the characteristic lengths for each of the fuels, are given in Table A1-2. The characteristic geometric length for the present arrangement is $L_{sp} \approx 1.5$ centimeters. On the basis of our characteristic lengths analysis, we have concluded that a single performance model (A1) can be used to predict the performance of the Texaco engine for a large number of fuels of practical interest including methanol, gasoline,

TABLE A1-1 PHYSICAL PROPERTIES OF THE FUELS UNDER CONSIDERATION

Property \ Fuel	Methanol	Gasoline	JP-4	Diesel	Wide-Range Distillate
Chemical Formula	CH_3OH	(C_8H_{16})		$(C_{12}H_{26})$	
Density, gm/cc	0.796	0.76	0.77	0.82	0.785
Absolute Viscosity, centipoise	0.46	0.40	0.89	3.61	50
Surface Tension, dynes/cm	21	20	21	23	21.5
Boiling Range, ^0C					
Initial Boiling Point		40	60	200	43
50%	65	100	160	275	181
Final Boiling Point		200	250	350	324
Heat of Vaporization, cal/gm	262	64	50	39	55
Lower Heating Value					
per unit mass, cal/gm	4,794	10,260	10,340	10,420	10,500
per unit volume, cal/cc	3,806	7,798	7,962	8,544	8,243

TABLE A1-2 CHARACTERISTIC LENGTH CONSIDERATIONS FOR VARIOUS FUELS

Length / Fuel	Break-up and Deceleration		Vaporization	Momentum
Methanol	$Z = 0.0047$ Rey. $\geq$ 18,860 $V_{initial} \geq 1{,}920$ cm/sec	~150 drop diameter ~1.5 mm	$B = 0.386$ $\lambda_s = 1.96 \times 10^{-4}$ cm^2/sec $\tau_{ev} = 0.85$ msec	$L_{mom} > L_{sp}$ [but not very large]
Gasoline	$Z = 0.0043$ Rey. $\geq$ 20,255 $V_{initial} \geq 1{,}900$ cm/sec	"	$B = 1.032$ $\lambda_s = 4.46 \times 10^{-4}$ cm^2/sec $\tau_{ev} = 0.34$ msec	$L_{mom} \simeq L_{sp}$
JP - 4	$Z = 0.0093$ Rey. $\geq$ 10,930 $V_{initial} \geq 2{,}220$ cm/sec	"	$B = 0.772$ $\lambda_s = 3.55 \times 10^{-4}$ cm^2/sec $\tau_{ev} = 0.47$ msec	$L_{mom} \simeq L_{sp}$
Diesel	$Z = 0.0348$ Rey. $\geq$ 3,800 $V_{initial} \geq 3{,}000$ cm/sec	"	$B = 0.39$ $\lambda_s = 1.92 \times 10^{-4}$ cm^2/sec $\tau_{ev} = 0.87$ msec	$L_{mom} \simeq L_{sp}$
Wide-Range Distillate	$Z = 0.51$ Rey. $\geq$ 444 $V_{initial} \geq 4{,}962$	"	$B = 0.639$ $\lambda_s = 3.01 \times 10^{-4}$ cm^2/sec $\tau_{ev} = 0.55$ msec	$L_{mom} \simeq L_{sp}$

JP-4, diesel and a wide-range distillate since:

(a) The injection velocities used in practice are higher than those required for "immediate" break-up of the jet.

(b) Deceleration of droplets is rapid - within a millimeter or so from the nozzle tip.

(c) Most of the fuel evaporates by the time it reaches the spark plug.

In addition since the momentum length and L_{sp} are comparable, we also conclude that the effect of the cross-flow has to be included in the jet mixing analysis.

Jet Model - From the characteristic lengths analysis, we conclude that the fuel jet breaks into droplets near the nozzle orifice and that the relative velocity of droplets in the jet flow is small. A quasi-steady jet model, similar to the one used by Rife and Heywood (A2) is used to analyze the motion of the fuel jet. The model is based on the turbulent entrainment assumptions of Hoult and Weil (A8). In this analysis, the rates of entrainment for turbulent plumes introduced by Hoult and Weil have been modified to include the effects of large density variations, as suggested by Ricou-Spalding (A9) and Escudier (A5). The jet geometry is shown in Figure A1-2. The governing equations for the jet motion are:

Conservation of Mass:

$$\frac{d}{ds}(\rho\pi b^2 u) = \left(\frac{\rho}{\rho_\infty}\right)^{1/2} 2\pi b\rho_\infty \left[\alpha|u - V_t| + \beta|V_n|\right] \qquad \text{(A1-13)}$$

Conservation of Momentum:

Horizontal component:

$$\frac{d}{ds}(\pi b^2 u^2 \sin\theta) = V\cos\phi \frac{d}{ds}(\pi b^2 u) \qquad \text{(A1-14)}$$

Vertical Component:

$$\frac{d}{ds}(\pi b^2 u^2 \sin\theta) = V\sin\phi \frac{d}{ds}(\pi b^2 u) \qquad \text{(A1-15)}$$

Conservation of Fuel:

$$\frac{d}{ds}(\pi b^2 u x_f) = 0$$

where b = jet radius
s = distance along the jet trajectory
u = jet velocity
V = cross-flow velocity
V_n = component of V normal to u
V_t = component of V parallel to u
x_f = mass fraction of fuel in the jet

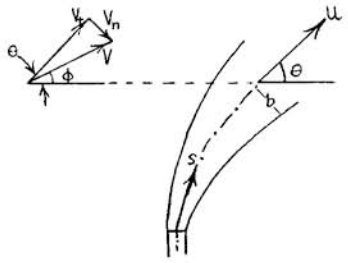

Fig.A1-2 - Geometry of the jet

α = entrainment parameter for the parallel flow
β = entrainment parameter for the normal flow
θ = inclination of jet to horizontal
ρ = mixture density in the jet
ρ_∞ = density of the surrounding gas
ϕ = inclination of V to horizontal

With these governing equations, the problem reduces to an initial value problem and knowing the initial conditions of the fuel jet and the nature of the cross-flow, the equations can be numerically integrated to obtain the space-time history of the jet.

We have chosen to use the entrainment coefficients of Hoult and Weil (A3) of $\alpha = 0.11$ and $\beta = .6$.

For the Texaco nozzle, a discharge coefficient of 0.61 appears to give reasonably good agreement between the theoretical predictions and experimental data.

REFERENCES

A1. B.C. Jain, J.C. Keck and J.M. Rife, "A Performance Model for the Texaco Controlled Combustion, Stratified Charge Engine," paper presented at 1976 Automotive Engineering Congress and Exposition, Detroit.

A2. J. Rife and J.B. Heywood, "Photographic and Performance Studies of Diesel Combustion with a Rapid Compression Machine," SAE Paper 740948.

A3. D.P. Hoult and W.C. Weil, "Turbulent Plume in a Laminar Cross Flow," Atmospheric Environment, Vol. 6, 1972, pp. 514-531. (Printed in Great Britain).

A4. J.P. Ricou and D.B. Spalding, "Measurement of Entrainment by Axial Symmetric Turbulent Jets," J. Fluid Mech., 9, 21 (1961).

A5. M.P. Escudier, "Aerodynamics of a Burning Turbulent Gas Jet in a Cross Flow," Combustion Science & Technology, April, 1972.

A6. M.K. Martin, S.M. Thesis, Mech. Engineering, M.I.T., (1975).

A7. A. Haenlein, "On the Disruption of a Liquid Jet," Forsch Arb. Geb. Ing. Wes. 1931 Vol. 2, (#4, April).

A8. C. Weber, "On the Disruption of a Liquid Jet," Z. Angew. Math. Mech. 1931,

Vol. 11, (#2, April).

A9. W.V. Ohnesorge, "The Formation of Drops from Nozzles and the Disruption of a Stream of Liquid," Z. Angew, Math. Mech., 1936, Vol. 16 (#1, December).

A10. Burt and Troth, "Penetration and Vaporization of Diesel Fuel Sprays," Diesel Engine Combustion, Inst. Mech. Engrs., 1969-70, paper #15.

A11. J.M. Beer and N.A. Chigier, "Combustion Aerodynamics," John Wiley and Sons, 1972.

A12. W.E. Ranz and W.P. Marshall, "Evaporition from Drops," Chem. Eng. Progress, 48 pp. 141-146 and 173-180 (1952).

APPENDIX II

The Plume Geometry oodel and Heat Transfer - During and after rapid combustion, the charge inside the cylinder consists of a plume of hot burned gas surrounded by an unburned gas mixture. Parts of the walls of the combustion chamber are in contact with the hot, burned gas plume and the remaining sections are in contact with relatively cold unburned gas mixture. The total heat transfer area can be divided into two parts and a plume geometry model is required to determine the two areas for heat transfer. In addition, the computations for the rate of entrainment of gas mixture by the plume during the mixing-dominated phase of combustion require knowledge of the surface area of the plume. The model for computing the plume geometry draws partly on the combustion movies taken on the Texaco engine. These high speed combustion movies were taken at a frequency of about 16,000 frames per second. During the initial phases of rapid combustion, the development of the plume can be clearly observed on the combustion movies and it appears that the plume starts at the spark plug and is swept around in the flow field induced by high swirl rates. After the initial phases, the intense radiation from the flames distorts the apparent plume geometry.

The Model - We assume that the plume starts at the spark plug and is swept around in swirling air flow. We assume that the plume grows in a uniform manner laterally around the spark-plug radius (R) until growth in any direction is impeded by the presence of chamber walls. The contact with chamber walls in any direction is assumed to prevent further growth in that direction without affecting the rate of growth in any other direction.

The plume geometry model is then divided into three phases as shown in Figure (A2-1); and Figure (A2-2) is a schematic which defines all the symbols to be used in the model. During the first stage of combustion the burned gas plume does not touch any of the combustion chamber walls and all heat transfer areas are in contact with relatively cold unburned gas mixture. The plume is considered to be a section of a torus. As combustion proceeds, an ever increasing part of the total combustion chamber wall area comes in contact with the burned gas plume and the plume is assumed to consist of either two hollow discs on top of each other (Stage II)or as two solid discs on top of each other (Stage III) as shown in Figure (A2-1).

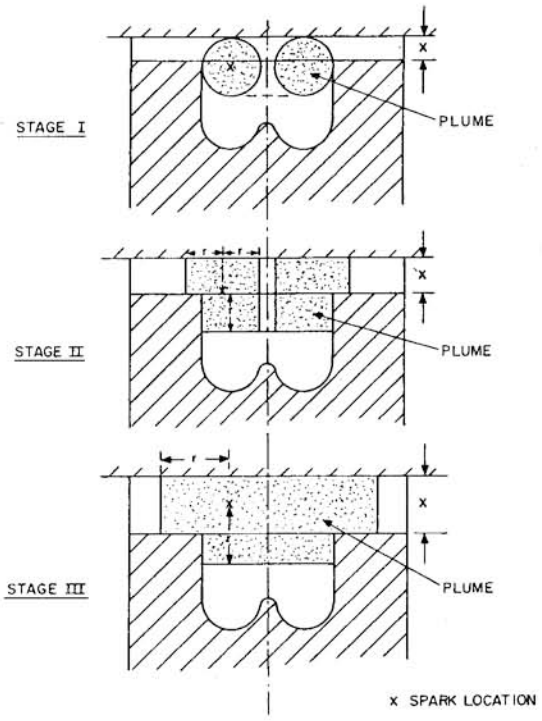

Fig.A2-1 - Various stages in the plume geometry model

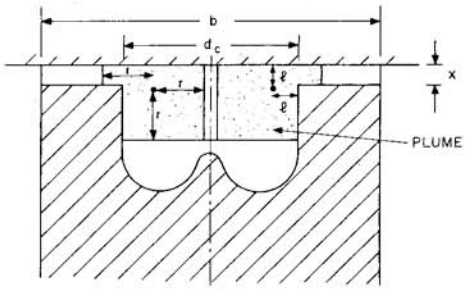

Fig.A2-2 - Schematic for plume geometry model

Stage 1: The boundaries of the three stages are defined in terms of the volume occupied by the burned gas plume. The first stage covers the initial development of the plume and ends when the cross sectional radius, r, of the torus becomes equal to ℓ, or at the time that the plume approaches the chamber walls. Thus, Stage 1 covers the region when

$$0 \leq V_b \leq V_1$$

where

$$V_1 = 2\pi^2(\frac{d_c}{2} - \ell)\ell^2 \qquad (A2\text{-}1)$$

is the volume of a torus with inner radius $(\frac{d_c}{2} - 2\ell)$ and outer radius $\frac{d_c}{2}$.

The volume of the torus, in this stage, is given as

$$V_b = 2\pi^2(\frac{d_c}{2} - r)r^2 \qquad (A2\text{-}2)$$

and r is the characteristic radius of the plume. During Stage 1, all the walls of the chamber are in contact with unburned gas mixture so that

$$A_b = 0 \qquad (A2\text{-}3)$$

$$A_a = A_T$$

where

$$A_T = \frac{\pi b^2}{4} + \pi b\, x + \frac{\pi}{4}(b^2 - d_c^2) + A_{cup} \qquad (A2\text{-}4)$$

The surface area of the plume is given by

$$S_e = 4\pi^2 Rr \qquad (A2\text{-}5)$$

where

$$R = (\frac{d_c}{2} - \ell)$$

Stage II: The plume is assumed to consist of two hollow discs on top of each other (see Figure A2-1). This stage ends when the characteristic radius r of the plume equals R, so that Stage II covers the region

where

$$V_1 < V_b \leq V_2 \qquad (A2\text{-}6)$$

Where

$$V_2 = 4\pi x\,(\frac{d_c}{2} - \ell)^2 + \frac{\pi}{4}\,(\frac{d_c}{2} - x)\,d_c^2 \qquad (A2\text{-}7)$$

and the characteristic radius of the plume is obtained by recognizing that the volume during this stage is given by

$$V_b = 4\pi\, x\, Rr + \pi[(\ell - x) + r]\,[(\frac{d_c}{2})^2 - (R - r)^2] \qquad (A2\text{-}9)$$

The wall areas in contact with hot, burned gas plume and relatively cold gas mixture are:

$$A_b = 4\pi\, Rr + \pi d_c(r + \ell - x) + \pi[(R + r)^2 - (\frac{dc}{2})^2] \qquad (A2\text{-}9)$$

$$A_a = A_T - A_b$$

where A_T is given by (A2-4). The surface area of the plume for entrainment is given as

$$S_e = 2\pi(R + r)\, x + \pi(r + \ell)[3(R - r) + \frac{d_c}{2}] \qquad (A]\text{-}10)$$

Stage III: The plume is considered to consist of two solid discs on top of each other (see Figure A2-1) and this phase ends when the plume touches cylinder walls and the characteristic radius r equals (b/2-R). The period covered in this stage is given by

$$V_2 < V_b \leq V_3$$

where

$$V_3 = \frac{\pi}{4}\, x\, b^2 + \frac{\pi}{4}\,[\frac{b}{2} - R + \ell - x]d_c^2 \qquad (A2\text{-}11)$$

and the characteristic radius of the plume, r, is obtained by the relationship

$$V_b = \pi x(R + r)^2 + \frac{\pi}{4}(r + \ell - x)d_c^2 \qquad (A2\text{-}12)$$

The areas for heat transfer are

$$A_b = \pi(R + r)^2 + \pi[(R + r)^2 - (\frac{d_c}{2})^2]\,\pi d_c(r + \ell - x) \qquad A2\text{-}13)$$

and $$A_a = A_T - A_b$$

where A_T is again given by (A2-4). The surface area of the plume for entrainment is given as

$$S_e = 2\pi(R + r)x + \frac{\pi d_c^2}{4} \qquad (A2\text{-}14)$$

At the end of the third period the volume V_3 may not equal the instantaneous volume of the cylinder because of the cup in the piston. Hence

for $V_3 < V_b < V$

$$A_b = (A_b)_3 + [A_T - (A_b)_3]\,[\frac{V_b - V_3}{V - V_3}]^{2/3} \qquad (A2\text{-}15)$$

$$A_a = A_T - A_b$$

and

$$S_e = (S_e)_3 \left[\frac{V - V_b}{V - V_3}\right]^{2/3}$$

where $(A_b)_3$ and $(S_e)_3$ are the values of A_b and S_e at the end of Stage III

$$(A_b)_3 = \frac{\pi b^2}{4} + \frac{\pi}{4}(b^2 - d_c^2) + \pi d_c\left(\frac{b}{2} - R + \ell - x\right) \quad \text{(A2-17)}$$

and

$$(S_e)_3 = \frac{\pi d_c^2}{4} \quad \text{(A2-18)}$$

The plume geometry model is required only during rapid combustion and mixing-dominated phases since the plume and the unburned gas mixture co-exists only during this period. Before the rapid combustion phase, the charge consists of unburned gas mixture alone while after the end of mixing dominated phase, the charge consists of burned gas only.

Heat Transfer Equation: The heat transfer equation is given as:

$$Q = h_a A_a (T_a - T_w) + h_b A_b (T_b - T_w) \quad \text{(A2-19)}$$

where

$$h_a = 7014\, b^{-0.2} p^{0.8} T_a^{-0.53} \left[C_1\left(\frac{SN}{30}\right) + 100 C_2 \frac{VT_o}{P_o V_o}(p - p_{is}) + (V_s)_a\right]^{0.8} \quad \text{(A2-20)}$$

and

$$h_b = 7014\, b^{-0.2} p^{0.8} T_b^{-0.53} \left[C_1\left(\frac{SN}{30}\right) + 100 C_2 \frac{VT_o}{V_o V_o}(p - p_{is}) + (V_s)_b\right]^{0.8} \quad \text{(A2-21)}$$